SLICE EMITTANCE MEASUREMENTS AT SPARC PHOTOINJECTOR WITH A RF DEFLECTOR

C. Vaccarezza, D. Alesini, E. Chiadroni, G. Di Pirro, M. Ferrario, L. Ficcadenti, D. Filippetto, G. Gatti, B. Marchetti, E. Pace, INFN-LNF, Frascati (Roma), Italy
A. Cianchi, INFN-Roma Tor Vergata, Roma, Italy
A. Mostacci, University La Sapienza, Roma, Italy.

Abstract

The SPARC photoinjector is a R&D facility performing beam dynamics studies and driving a SASE-FEL. The RF deflector, completely designed and built by the SPARC team, allows measurements of the longitudinal properties of the beam bunch. Using it and the well know technique of the quadrupoles scan, the slice emittance has been measured. We report the experimental setup description together with the first measurement results.

INTRODUCTION

The goal of the SPARC R&D facility [1] is to produce a high brightness electron beam able to drive a SASE-FEL in the visible light and exploring all the most critical issues of the future X-ray source subsystems. The stringent FEL experiment requirements on the normalized emittance, both projected and “slice”, put a strong relevance on the experimental measurement of this beam feature. For this purpose a diagnostic beamline has been equipped at SPARC between the photoinjector and the undulators where a combined setup of a RF deflector cavity and a bending dipole is provided to fully characterize the six-dimension phase space of the photoinjector output beam. In this paper the slice emittance measurement with the RF deflector is described together with the preliminary results.

EXPERIMENTAL SETUP

The SPARC photoinjector consists of a 1.6-cell RF gun of the BNL/UCLA/SLAC type [2] operating at S band (2856 MHz), with a Cu incorporated metallic photocathode; it generates a 5 MeV electron beam. Three accelerating sections follow, S-band TW, raising the energy up to ≈150MeV. The M. Ferrario working point [3] is adopted for the beam transverse emittance compensation at the end of the SPARC linac. Downstream the third accelerating section a diagnostic beamline is located: a layout of the magnets and measurement flags used for the longitudinal and transverse phase space characterization is reported in Fig. 1. The longitudinal beam profile is measured powering the RF deflector and directly analyzing the image produced by the beam on the flag F1 while the complete longitudinal phase space is reconstructed using the RF deflector in combination with the dipole magnet, and analyzing the image produced by the beam on the flag FD1. Using the RF beam deflection in the vertical plane the horizontal slice emittance can be measured either on the transfer lines or on the dogleg, at the flags F1 or FD3, respectively. The last two quadrupoles after the linac sections, QT2 and QT3, are used for the quadrupole scan. In Fig. 1 the schematic layout of the beamline is reported.

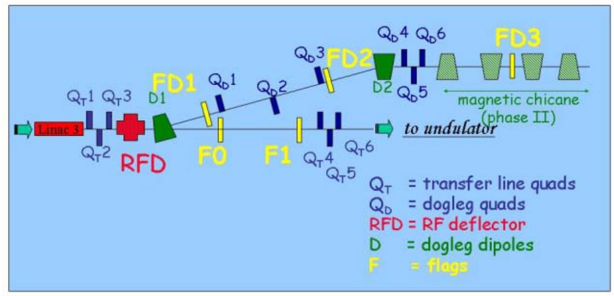

Figure 1: SPARC diagnostic beamline schematic layout

RF Deflector

The SPARC RF deflector developed at SPARC is a 5-cell SW reaching a maximum transverse deflecting voltage of more than 3*MW* with an input power of nearly 2*MW* [4]. The main parameters and dimensions are reported in Table 1, while in Fig. 2 a picture of the deflector installed in the diagnostic beamline is shown besides a 3D sketch of a quarter of the structure.

The transverse distribution of the bunch at the screen position is the superposition between the deflected beam size and the vertical dimension of the bunch slices at the flag position (σ_y), as illustrated in Fig. 3. The rms resolution length (L_{res}) can be defined as the bunch length that gives, on the flag, a vertical spot exactly equal to σ_y. When a simple drift space is provided between the RF

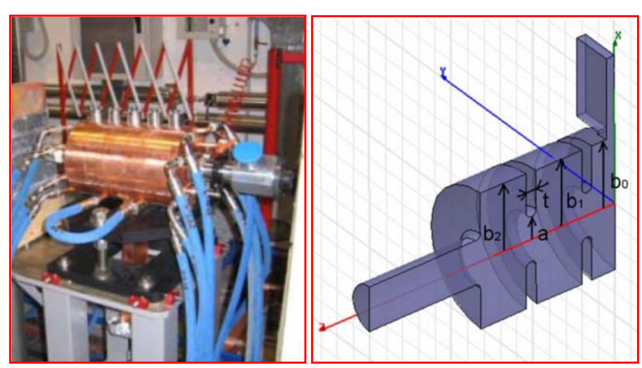

Figure 2 picture of the deflector as installed in the SPARC beamline and a 3D sketch of a quarter of the structure.

deflector and the considered screen, the achievable measurement resolution follows from (our case L=3.90m):

$$L_{res} \cong \frac{\sigma_y \, cE/e}{\omega_{RF} L V_\perp} = \frac{cE/e\sqrt{\varepsilon_y \beta_{y\_defl}}}{\omega_{RF} L V_\perp} \qquad (1)$$

Table 1: SPARC RF deflector dimensions and parameters.

Dimensions (mm)	Parameters	Dimensions (mm)	Parameters
b_2	60.92	b_2	60.92
b_1	59.93	b_1	59.93
b_0	60.04	b_0	60.04
a	20	a	20

MEASUREMENT PROCEDURE

RF Deflector Calibration

In order to better evaluate the scaling factor between the bunch longitudinal length and its vertical dimension on the screen, the RF-deflector deviation is calibrated by measuring the beam centre position vs. the varying RF-deflector phase: from the curve slope the scaling factor between the longitudinal and the vertical dimension is obtained. Applying $V_\perp = 1.8kV$, i.e. $P_{RF} = 700kW$, we obtain the scaling factor $f = 0.38(longmm)/mm$. The zero-crossing phase is provided by the centroid position previously determined with the RF deflector switched off, and the bunch length can be measured.

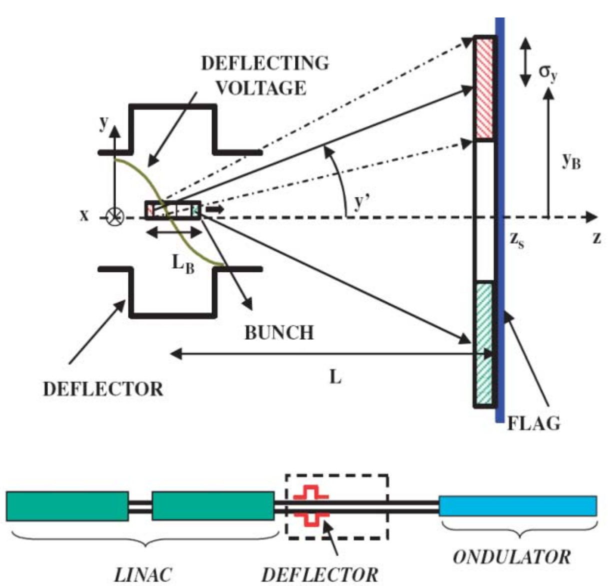

Figure 3: Bunch length measurement schematic setup using an RF deflector.

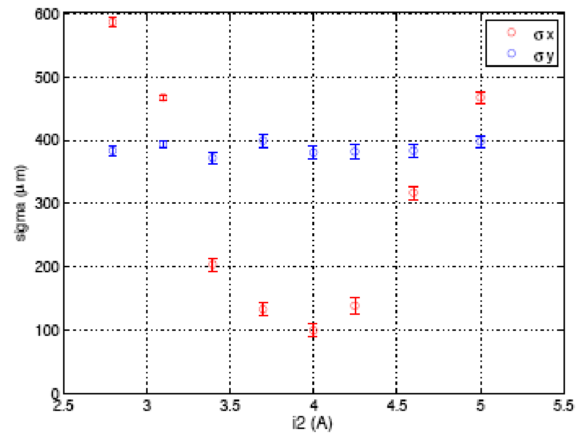

Figure 4 : Transverse beam dimensions as function of the second quad power supply applied current.

Quadrupole Scan

The quadrupole scan is performed with the two quadrupoles placed upstream the RF- deflector in order to keep constant the vertical dimension of the beam, with a typical value of $\sigma_y \approx 400\ \mu m$ and a stability of ≈0.07% as can be seen in Fig. 4 where the beam transverse dimensions are plotted as recorded during a q-scan with the RF-deflector switched off. Twenty images are averaged for each current step.

DATA ANALYSIS

The twenty images group is off-line analyzed performing for each one the region of interest, (ROI) selection. This is illustrated in Fig. 5 where from left to right the YAG screen contour is excluded from the analysis. The background in this case is not filtered due to negligible contribution of the dark current.

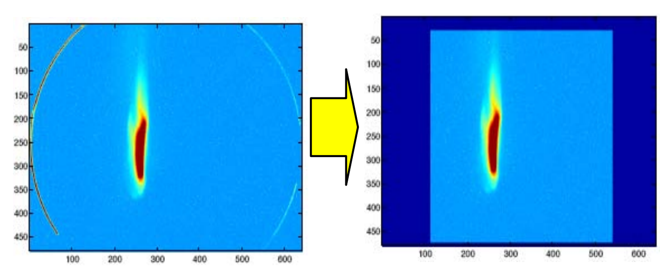

Figure 5: From each one of the recorded pictures the region of interest is selected using the maximum/3 threshold criterion.

For each quad-current step the beam vertical profile is obtained averaging over the twenty image group; the signal baseline is selected above the maximum/3 threshold, see Fig. 6.

The horizontal profile signal cleaning is performed with the same algorithm employed for the emittance-meter data analysis [5]: the initial value for the baseline and rms width is estimated at first, defining the ROI window, centered on the maximum of the distribution. The baseline is then calculated by averaging the portion of distribution out of the window, while the initial value for the rms width is calculated over the portion of distribution inside it. The fit results are then used to adjust the original

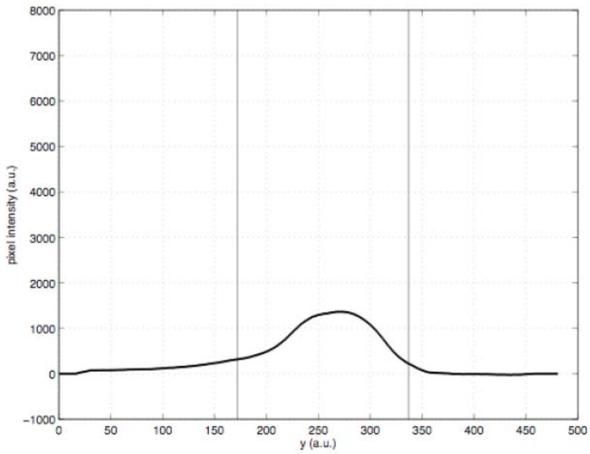

Figure 6: Vertical profile selection of the image and its footprint on the particle distribution

profile by subtracting the baseline and limiting the ROI to ± 5 times the rms width around the mean. Noise suppression of the profile curve is obtained by an iterative procedure which computes the rms value, then shrinks the region of interest down to ±3 times the rms and so on. The procedure stops when the new values match the result of the previous iteration. The algorithm converges typically after 4–5 iterations.

EXPERIMENTAL RESULTS

First slice emittance measurements have been performed on a 300pC beam, with E=145 MeV The vertical rms dimension was σ_y=400 µm, that with the measured calibration factor, corresponds to L_{res}= 150 µm for a measured total bunch length $L_b \approx 2.22$ mm. For the first analysis the considered slice length is ≈ 300 µm corresponding to a total of six slices, and then 13 slices for a slice length of ≈ 150 µm. The charge distribution is reconstructed to check the beam portion excluded from the analysis taking into account the signal threshold of maximum/3: the 78% of the beam results selected. The reconstructed slice emittance is shown in Fig. 7 for the six slices analysis, and in Fig. 8 for the thirteen slices The lowest value obtained are ε_{nx}=1.4 ± 0.1 and ε_{nx}=1.3 ± 0.1 for six and thirteen slices respectively, in reasonable agreement the one with each other.

CONCLUSIONS

The first slice emittance measurement results obtained at SPARC have been reported together with a brief description of the whole measurement data taking and analysis process. Even though not so relevant concerning the photoinjector optimization, nevertheless they represent a good test for the whole high energy diagnostic setup provided at the SPARC R&D facility, after the first experience with the emittance-meter [5]

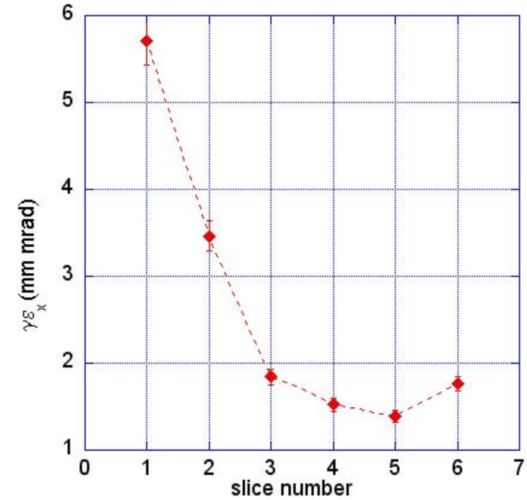

Figure 7: Horizontal slice emittance reconstruction with six slices considered, L_{slice}≈300 µm

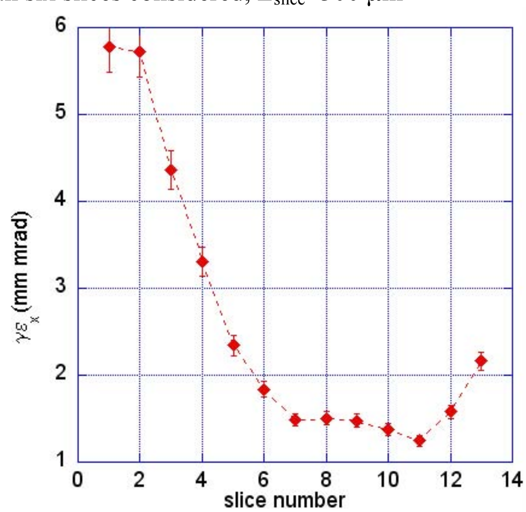

Figure 8: Horizontal slice emittance reconstruction with thirteen slices considere, L_{slice}≈150 µm.

REFERENCES

[1] http://www.lnf.infn.it/acceleratori/sparc/

[2] D.T. Palmer, The next generation photoinjector, Ph.D. Thesis, Stanford University, 1998.

[3] M. Ferrario et al., "HOMDYN study for the LCLS RF photoinjector", SLAC-PUB-8400, (2000

[4] D. Alesini et al., Science Direct, Nucl. Jnstr. Meth. Jn Phys. R. A 568 (2006), 488-502

[5] A. Cianchi et al., Phys. Rev. ST Accel. Beams **11,** 032801 (2008)